

Four-spin cyclic exchange in spin ladder cuprates

Carmen J. Calzado,¹ Coen de Graaf,² Esther Bordas,² Rosa Caballol,² and Jean-Paul Malrieu³¹Departamento de Química Física, Universidad de Sevilla, 41012 Sevilla, Spain²Departament de Química Física i Inorgànica, Universitat Rovira i Virgili, 43005 Tarragona, Spain³Laboratoire de Physique Quantique, IRSAMC, Université Paul Sabatier, 31062 Toulouse-Cedex, France

(Received 8 January 2003; published 28 April 2003)

The four-spin cyclic exchange term J_{ring} of three spin-ladder cuprates (SrCu₂O₃, Sr₂Cu₂O₅, and CaCu₂O₃) has been calculated from *ab initio* quantum chemistry calculations. For the first two compounds, a non-negligible cyclic exchange is found, approximately 20% of the magnetic coupling across the rungs, J_{\perp} , and always larger than the value obtained for two-dimensional La₂CuO₄ system. In the case of CaCu₂O₃, the J_{ring} value is quite small, due to the folding of the Cu-O-Cu rung angle, but the J_{ring}/J_{\perp} ratio is also 0.2 as in the two other systems.

DOI: 10.1103/PhysRevB.67.132409

PACS number(s): 75.30.Et, 71.27.+a, 71.70.Gm, 75.50.Ec

Spin-ladder cuprates constitute an active research field in the last decade.^{1,2} They can be viewed as intermediates between the one-dimensional (1D) antiferromagnets and the still controversial two-dimensional (2D) square lattices. Ladders composed of Cu and O are specially interesting due to their proximity to high- T_c cuprates. Their magnetic properties depend on the number of legs. Even-legged ladders show a spin gap excitation, whereas odd-legged ladders are gapless and behave as a 1D spin chain.^{1,2} They also present different properties regarding hole doping. It has been suggested that even-legged spin ladders become superconductors upon hole doping, which has been confirmed experimentally³ in the two-legged ladder Sr_{14-x}Ca_xCu₂₄O₄₁ under high pressure.

The magnetic properties of these compounds are controlled by the effective magnetic coupling constant J , related with the amplitude of the interactions between the spin moments of the Cu²⁺ ions. Different J constants can be defined, as shown in Fig. 1. The two most important are the coupling along the legs, J_{\parallel} , and across the rungs, J_{\perp} . The ratio J_{\perp}/J_{\parallel} is controversial since the interpretation of different experimental data has led to estimates ranging from spatially isotropic, $J_{\perp}/J_{\parallel}=1$, to strongly anisotropic couplings, $J_{\perp}/J_{\parallel}=0.5$. The strong spatial anisotropy $J_{\perp}/J_{\parallel}=0.5$ is in contradiction with geometrical considerations. Since the Cu-O-Cu bonds are quite similar, the exchange pathways are expected to be equivalent, and so, $J_{\parallel}\sim J_{\perp}$. The theoretical calculations of Mizuno, Tohyama, and Maekawa,⁴ and de Graaf *et al.*⁵ are in agreement with these considerations.

It should be noted that most of the available J_{\perp} and J_{\parallel} values have been obtained by fitting the experimental data onto a model Heisenberg Hamiltonian, containing just two-body operators. As in the case of the 2D cuprates,⁶⁻¹⁰ some authors have recently suggested the necessity of introducing additional interactions in the model Heisenberg Hamiltonian to study the properties of the spin ladders. The most important are the diagonal coupling (second-neighbor interactions), the interladder exchange and, especially, the four-spin cyclic exchange (4SCE). In this context, de Graaf *et al.*⁵ have proposed that the omission of the interladder coupling in the analysis of experimental data for SrCu₂O₃ may be the reason that a ratio $J_{\perp}/J_{\parallel}\sim 0.5$ was obtained instead of $J_{\perp}/J_{\parallel}\sim 1$. However, the quantum Monte Carlo (QMC) simu-

lations of the temperature dependence of the magnetic susceptibility of Johnston *et al.*¹¹ do not confirm this hypothesis. The inclusion of a ferromagnetic interladder coupling, ($J_{inter}/J_{\parallel}=-0.1$), in their QMC simulations does not change the fitted $J_{\perp}/J_{\parallel}\sim 0.5$ ratio obtained for SrCu₂O₃.

Recently, Brehmer *et al.*¹² have analyzed the role of the 4SCE on the determination of coupling constants from ladder spectra. The 4SCE is a fourth-order term in the Hubbard model, involving the circulation of the electrons around the plaquette and scales as $80t^4/U^3$, t being the hopping integral and U the on-site Coulomb repulsion.^{13,14} The extended Heisenberg Hamiltonian containing the diagonal interactions and the 4SCE terms has the following form:

$$H = \sum_{\langle ij \rangle}^{legs} J_{\parallel} \left(S_i S_j - \frac{1}{4} \right) + \sum_{\langle ij \rangle}^{rungs} J_{\perp} \left(S_i S_j - \frac{1}{4} \right) + \sum_{\langle ij \rangle}^{NNN} J_{diag} \left(S_i S_j - \frac{1}{4} \right) + \sum_{\langle ijkl \rangle} J_{ring}^{ijkl} \left[(S_i S_j)(S_k S_l) + (S_i S_l)(S_j S_k) - (S_i S_k)(S_j S_l) - \frac{1}{16} \right], \quad (1)$$

where the higher multiplet energy is set to zero, J_{\parallel} and J_{\perp} correspond to nearest-neighbor (NN) interactions, J_{diag} to the next nearest-neighbor (NNN) coupling, and J_{ring}^{ijkl} to the 4SCE terms; and the superscript refers to the type of cyclic interaction. Actually the introduction of J_{diag} (especially, if it is antiferromagnetic) implies that the NNN hopping t_{diag} is not negligible, and the circulation of the four electrons may involve the diagonal hopping. The physical content and origin of the three types of J_{ring} is schematized in Fig. 2.

It has been argued that a finite value of the ring exchange is necessary to reproduce the structure of the magnetic Raman spectrum for 2D insulating cuprates.^{7,9,10} In spin-ladder cuprates, Brehmer *et al.*¹² have concluded that the cyclic exchange has a large influence on the spin gap and, consequently, on the exchange constant values J_{\parallel} and J_{\perp} . A small amount of J_{ring} ($J_{ring}\approx 0.28J_{\perp}$) is consistent with $J_{\parallel}\approx J_{\perp}$ as expected from the geometrical structure. A similar result has been obtained by Matsuda *et al.*¹⁵ for the two-legged ladder La₆Ca₈Cu₂₄O₄₁. A reasonable fit to the experimental data is

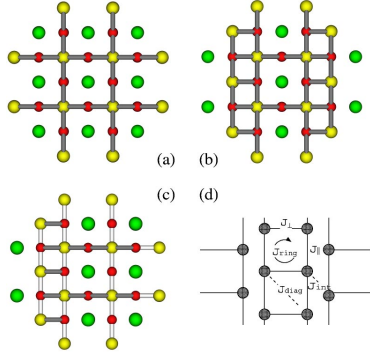


FIG. 1. Cu_4O_{12} plaquettes and first-neighbor TIP's environment models for (a) La_2CuO_4 , (b) SrCu_2O_3 and CaCu_2O_3 , and (c) $\text{Sr}_2\text{Cu}_3\text{O}_5$ compounds. Gray, small black, and big dark circles correspond, respectively, to Cu, O, and counterions atoms (Sr^{+2} , Ca^{+2} , or La^{+3}). The different types of exchange interactions in the spin ladders are shown in (d).

obtained when a finite cyclic exchange (30% of J_{\perp}) is included in the Hamiltonian, with $J_{\parallel} = J_{\perp} = -110$ meV. In the absence of this 4SCE, a fit of comparable quality is obtained with $J_{\perp} = -53$ meV and $J_{\parallel} = -106$ meV. So, it seems that the neglect of the 4SCE term could lead to the strong anisotropy found for spin-ladder cuprates.

It is the aim of this report to simultaneously determine all the effective interactions, appearing in Eq. (1), with special attention to the 4SCE term, by means of *ab initio* quantum chemical embedded cluster calculations. We report the amplitude of these operators for three spin-ladder compounds: SrCu_2O_3 , CaCu_2O_3 , and $\text{Sr}_2\text{Cu}_3\text{O}_5$; and compare the results with the values obtained for the 2D La_2CuO_4 system. A detailed analysis of the eigenvalues and wave functions of these systems enables us to determine the exchange interactions in a Cu_4O_{12} plaquette: the NN interactions, J_{\perp} and J_{\parallel} , the NNN interaction J_{diag} , and the 4SCE term, J_{ring} . This approach only depends on the quality of the approximation

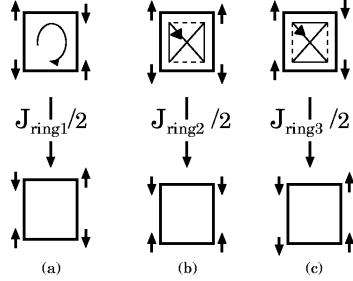


FIG. 2. Four-spin cyclic exchange couplings: (a) J_{ring1} , circular movement of the electrons, (b) J_{ring2} , simultaneous exchange along the legs, and (c) J_{ring3} , simultaneous exchange across the rungs.

of the exact wave functions obtained from the calculations and the correctness of the modeling.

The three systems here considered have different structural features. SrCu_2O_3 is a two-legged ladder, with a spin gap of 680 K.^{16,17} $\text{Sr}_2\text{Cu}_3\text{O}_5$ is a three-legged ladder without spin gap. The structure of CaCu_2O_3 is similar to that of SrCu_2O_3 , but the Cu-O-Cu bond angle in the ladder rungs equals 123° , and, therefore, the magnetic interaction along the rung is expected to be much weaker than in SrCu_2O_3 .

In all systems, a Cu_4O_{12} plaquette has been chosen, embedded in a set of optimized point charges placed at the lattice positions to model the crystalline environment (see Fig. 1). The Cu ions directly bonded to the cluster have been described by total ion potentials (TIP's) to avoid an artificial polarization of the oxygen orbitals. TIP's have been also employed to represent the Sr and Ca ions in the neighborhood of the cluster. The comparison of the cluster model and periodic calculations on related compounds has shown that this representation of the crystal is sufficient to accurately describe the type of interactions, subject of the present study.¹⁸ Details concerning the type of configuration interaction (CI) calculations performed and the basis set used can be found in Ref. 19.

The strategy to extract the effective 4SCE interaction in

TABLE I. The Heisenberg Hamiltonian on the basis of the model space for SrCu_2O_3 and CaCu_2O_3 . J_{r1} , J_{r2} , and J_{r3} correspond, respectively, to J_{ring1} , J_{ring2} , and J_{ring3} (see text).

$ a(\uparrow)b(\downarrow)c(\uparrow)d(\downarrow) $	$ a(\downarrow)b(\uparrow)c(\downarrow)d(\uparrow) $	$ a(\uparrow)b(\uparrow)c(\downarrow)d(\downarrow) $	$ a(\downarrow)b(\downarrow)c(\uparrow)d(\uparrow) $	$ a(\uparrow)b(\downarrow)c(\downarrow)d(\uparrow) $	$ a(\downarrow)b(\uparrow)c(\uparrow)d(\downarrow) $
$-J_{\parallel} - J_{\perp}$	$\frac{1}{2}J_{r1}$	$\frac{1}{2}J_{\parallel} + \frac{-J_{r1} - J_{r2} + J_{r3}}{8}$	$\frac{1}{2}J_{\parallel} + \frac{-J_{r1} - J_{r2} + J_{r3}}{8}$	$\frac{1}{2}J_{\perp} + \frac{-J_{r1} + J_{r2} - J_{r3}}{8}$	$\frac{1}{2}J_{\perp} + \frac{-J_{r1} + J_{r2} - J_{r3}}{8}$
$-J_{\parallel} - J_{\perp}$	$\frac{1}{2}J_{\parallel} + \frac{-J_{r1} - J_{r2} + J_{r3}}{8}$	$\frac{1}{2}J_{\parallel} + \frac{-J_{r1} - J_{r2} + J_{r3}}{8}$	$\frac{1}{2}J_{\perp} + \frac{-J_{r1} + J_{r2} - J_{r3}}{8}$	$\frac{1}{2}J_{\perp} + \frac{-J_{r1} + J_{r2} - J_{r3}}{8}$	$\frac{1}{2}J_{\perp} + \frac{-J_{r1} + J_{r2} - J_{r3}}{8}$
		$-J_{\parallel} - J_{diag}$	$\frac{1}{2}J_{r2}$	$\frac{1}{2}J_{diag} + \frac{J_{r1} - J_{r2} - J_{r3}}{8}$	$\frac{1}{2}J_{diag} + \frac{J_{r1} - J_{r2} - J_{r3}}{8}$
			$-J_{\parallel} - J_{diag}$	$\frac{1}{2}J_{diag} + \frac{J_{r1} - J_{r2} - J_{r3}}{8}$	$\frac{1}{2}J_{diag} + \frac{J_{r1} - J_{r2} - J_{r3}}{8}$
				$-J_{\perp} - J_{diag}$	$\frac{1}{2}J_{r3}$
					$-J_{\perp} - J_{diag}$

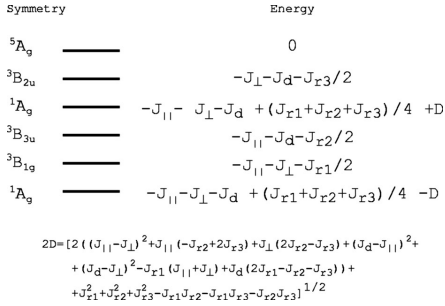


FIG. 3. Spectrum of the plaquette with one electron per Cu atom for SrCu_2O_3 and CaCu_2O_3 . For $\text{Sr}_2\text{Cu}_3\text{O}_5$, the parameter J_{\parallel} must be replaced by $(J_{\parallel}^{ext} + J_{\parallel}^{int})/2$. On the left, the corresponding symmetry of the different states in the D_{2h} group.

the CuO_2 layers of La_2CuO_4 has been reported in Ref. 19. For symmetry reasons, all the effective parameters in the plaquette (J , J_{diag} , and J_{ring}) can be evaluated from energy differences of the lowest states in the plaquette in La_2CuO_4 . In the case of the ladders, the number of unknown parameters is larger and the spectrum is no longer sufficient.

Let us consider the Cu_4O_{12} fragment in some more detail. The four unpaired electrons are located in the in-plane $d_{x^2-y^2}$ -type orbitals centered on each Cu atom. Calling a , b , c , and d the four magnetic orbitals (the rungs being a - b and d - c), the model space S is constituted by six neutral determinants with $M_s = 0$. Table I shows the extended Heisenberg Hamiltonian for four spins in a rectangular cluster on the basis of this model space. J_{ring_1} , J_{ring_2} , and J_{ring_3} concern the three types of 4SCE interactions present in the plaquette (Fig. 2): $J_{ring_1} = J_{ring}^{abcd}$ produces the circulation of all the spins in the plaquette, and $J_{ring_2} = J_{ring}^{adbc}$ and $J_{ring_3} = J_{ring}^{abdc}$ control, respectively, the simultaneous exchange of the spins in the two legs and across the two rungs. In the case of $\text{Sr}_2\text{Cu}_3\text{O}_5$, we can distinguish between the internal J_{\parallel}^{int} and the external leg J_{\parallel}^{ext} , and then, in the diagonal elements of the matrix, J_{\parallel} must be replaced by $(J_{\parallel}^{ext} + J_{\parallel}^{int})/2$.

The diagonalization of this matrix gives six eigenstates of different spin-space symmetries. Figure 3 shows the spectrum written on the basis of the parameters of the model

Hamiltonian. In all the cases, there are five energy differences. For SrCu_2O_3 and CaCu_2O_3 , there are six parameters; for $\text{Sr}_2\text{Cu}_3\text{O}_5$ there are seven. In order to avoid a bias in the determination of these sets of parameters, we use the effective Hamiltonian theory²⁰ to evaluate *all* parameters, instead of neglecting beforehand the presumably small secondary four-spin interactions J_{ring_2} and J_{ring_3} .

Our six eigenstates $|\psi_k\rangle$ (with energies E_k) have the largest projections on the model space S , with $P_S = \sum_{I \in S} |\phi_I\rangle\langle\phi_I|$ the projector on the model space. The Bloch effective Hamiltonian²⁰ can be written as

$$H^{Bloch} |P_S \psi_k\rangle = E_k |P_S \psi_k\rangle, \quad (2)$$

that is, the eigenvectors of this effective Hamiltonian are projections of the exact eigenvectors on the model space and their eigenenergies are the ones of the CI space. The spectral representation of the Bloch effective Hamiltonian is $H^{Bloch} = \sum_k |P_S \psi_k\rangle E_k \langle P_S \psi_k|$, where $|P_S \psi_k\rangle = S^{-1} |P_S \psi_k\rangle$ corresponds to the biorthogonal vectors, S being the overlap matrix between the projections $|P_S \psi_k\rangle$. Using this representation, it is possible to extract the values of the complete set of parameters.

The values obtained for the three spin ladders are presented in Table II, together with those extracted for the 2D La_2CuO_4 system.¹⁹ For SrCu_2O_3 and $\text{Sr}_2\text{Cu}_3\text{O}_5$, the J_{\perp}/J_{\parallel} ratio is closer to 1 than to 0.5, consistent with the geometrical structure of the ladders, and in agreement with the values obtained for SrCu_2O_3 from binuclear clusters.⁵ The NN interactions are always larger than for the 2D La_2CuO_4 compound. The diagonal interaction is antiferromagnetic, as in the 2D cuprates,^{8,21} with values around -15 meV. Regarding the cyclic terms, the parameters J_{ring_2} and J_{ring_3} are small in all cases. They are never larger than 4 meV and are not explicitly reported (hereafter, J_{ring} refers to J_{ring_1}). Notice, however, that this is an *a posteriori* information. The 4SCE is around 35 meV, significantly larger than for La_2CuO_4 . The J_{ring}/J_{\perp} ratio is 0.22 for both spin-ladder compounds, and it is consistent with that proposed by Matsuda *et al.*¹⁵ for $\text{La}_6\text{Ca}_8\text{Cu}_{24}\text{O}_{41}$ and the value suggested by Brehmer from numerical diagonalizations,¹² but smaller than those obtained for SrCu_2O_3 from the diagonalization of the d - p model Hamiltonian ($J_{ring}/J_{\perp} \sim 0.4$).⁴

The results for the CaCu_2O_3 system reflect the effect of the folding of the Cu-O-Cu rung angle. The coupling across the rungs is quite small, the bending of the Cu-O-Cu bond induces an unfavorable overlap of the active $d_{x^2-y^2}$ orbitals

TABLE II. Exchange parameters for SrCu_2O_3 , $\text{Sr}_2\text{Cu}_3\text{O}_5$, CaCu_2O_3 , and La_2CuO_4 . All parameters in meV, except U in eV.

	J_{\parallel}	J_{\perp}	J_{diag}	J_{ring}	J_{\perp}/J_{\parallel}	J_{ring}/J_{\perp}	U (eV)	$(J_{ring}^{ladder}/J_{ring}^{2D})^{pert}$	$(J_{ring}^{ladder}/J_{ring}^{2D})^{abinitio}$
SrCu_2O_3	-203	-157	-13	34	0.77	0.22	6.10 ^a	2.49	2.43
$\text{Sr}_2\text{Cu}_3\text{O}_5$	-195 (<i>ext</i>) -208 (<i>int</i>)	-177	-14	39	0.91 (<i>ext</i>) 0.85 (<i>int</i>)	0.22	6.10 ^a	2.78	2.79
CaCu_2O_3	-147	-15	-0.2	4	0.10	0.26	6.60 ^a	0.16	0.29
La_2CuO_4	-124	-124	-6.5	14	1.00	0.11	7.31 ^b	1.0	1.0

^aReference 24.

^bReference 23.

and the bridging oxygen ones. On the other hand, the J_{\parallel} value is -147 meV, larger than the NN coupling in 2D cuprates, and in good agreement with the estimations coming from magnetic susceptibility and neutron diffraction²² ($J_{\parallel} \sim -167 \pm 25$ meV). Both the NNN interaction and the 4SCE are also affected by the folding. However, the J_{ring}/J_{\perp} ratio is 0.26, similar to those obtained for the two other ladder compounds, and larger than the value reported for 2D cuprates.

As mentioned above, the 4SCE is a fourth-order term, scaling as $80t^4/U^3$. The perturbation theory second-order contribution to the magnetic coupling takes the form $J = -4t^2/U$. The perturbative expression for the 4SCE can be written as $J_{ring}^{pert} = 80r_{\perp}^2 t_{\parallel}^2 / U^3 = 5J_{\perp} J_{\parallel} / U$, and the perturbative $J_{ring}^{ladder}/J_{ring}^{2D}$ ratio is

$$\frac{J_{ring}^{ladder}}{J_{ring}^{2D}} = \frac{J_{\perp} J_{\parallel}}{J_{2D}^2} \frac{U_{2D}}{U_{ladder}}. \quad (3)$$

Table II reports the perturbative estimates of the $J_{ring}^{ladder}/J_{ring}^{2D}$ ratio, together with the on-site Coulomb repul-

sion, determined from *ab initio* quantum chemistry calculations on embedded binuclear clusters (Ref. 23 for the 2D cuprates and Ref. 24 for the ladders). An excellent agreement between the perturbative and the *ab initio* ratios is observed. (A similar behavior has been found for the perturbative estimates of J_{ring_2} and J_{ring_3} as will be shown elsewhere.²⁴) We can conclude that the larger values found for the 4SCE term in the spin-ladder cuprates reflect the enlargement of the NN coupling constants and the reduction of the on-site repulsion U with respect to the 2D cuprates. The NN coupling constant depends on t and U . Both parameters are affected by the changes in the Madelung potential and the different polarization effects in the ladder compounds in comparison to the 2D La_2CuO_4 compound. A detailed analysis of these effects will be given in a forthcoming paper.²⁴

Financial support has been provided by the Spanish Ministry of Science and Technology (Project No. PB98-1216-CO2-02), the DURSI of the Generalitat de Catalunya (Grant No. SGR01-00315), and the Catalan-French scientific cooperation (Grant No. PICS2001-13).

-
- ¹E. Dagotto and T.M. Rice, *Science* **271**, 618 (1996).
²T.M. Rice, *Z. Phys. B* **103**, 165 (1997).
³H. Takahashi *et al.*, *Physica B* **237-238**, 112 (1997).
⁴Y. Mizuno, T. Tohyama, and S. Maekawa, *Phys. Rev. B* **58**, R14 713 (1998); *J. Low Temp. Phys.* **117**, 389 (1999).
⁵C. de Graaf *et al.*, *Phys. Rev. B* **60**, 3457 (1999).
⁶M. Takahashi, *J. Phys. C* **10**, 1289 (1977).
⁷M. Roger and J.M. Delrieu, *Phys. Rev. B* **39**, 2299 (1989).
⁸H. Schmidt and Y. Kuramoto, *Physica C* **167**, 263 (1990).
⁹Y. Honda, Y. Kuramoto, and T. Watanabe, *Phys. Rev. B* **47**, 11 329 (1993).
¹⁰J. Lorenzana, J. Eroles, and S. Sorella, *Phys. Rev. Lett.* **83**, 5122 (1999).
¹¹D.C. Johnston *et al.*, cond-mat/0001147 (unpublished).
¹²S. Brehmer *et al.*, *Phys. Rev. B* **60**, 329 (1999).
¹³J.-P. Malrieu and D. Maynau, *J. Am. Chem. Soc.* **104**, 3021 (1982).
¹⁴A.H. MacDonald, S.M. Girvin, and D. Yoshioka, *Phys. Rev. B* **37**, 9753 (1988).
¹⁵M. Matsuda *et al.*, *Phys. Rev. B* **62**, 8903 (2000).
¹⁶K. Ishida *et al.*, *J. Phys. Soc. Jpn.* **63**, 3222 (1994).
¹⁷M. Azuma *et al.*, *Phys. Rev. Lett.* **73**, 3463 (1994).
¹⁸D. Muñoz, I. de P.R. Moreira, and F. Illas, *Phys. Rev. B* **65**, 224521 (2002).
¹⁹C.J. Calzado and J.-P. Malrieu, *Eur. Phys. J. B* **21**, 375 (2001); *Phys. Rev. B* **63**, 214520 (2001).
²⁰C. Bloch, *Nucl. Phys.* **B6**, 329 (1958).
²¹J.F. Annett *et al.*, *Phys. Rev. B* **40**, 2620 (1989).
²²V. Kiryukhin *et al.*, *Phys. Rev. B* **63**, 144418 (2001).
²³C.J. Calzado *et al.*, *J. Chem. Phys.* **116**, 3985 (2002).
²⁴E. Bordas *et al.* (unpublished).